

Homing Strategy for a 4RRR Parallel Kinematic Machine

WANG Liping, LIU Dawei*, and LI Tiemin

Department of Precision Instruments and Mechanology, Tsinghua University, Beijing 100084, China

Received May 26, 2010; revised January 23, 2011; accepted January 26, 2011; published electronically January 28, 2011

Abstract: Returning home is the most important process of a parallel kinematic machine (PKM) with incremental encoders. Currently, most corresponding articles focus on the accuracy of homing process, and there lacks the investigation of the operation's safety. For a 4RRR PKM, all servoaxes would be independently driven to their zero positions at the same time based on the traditional homing mode, and that can bring serious interfere of the kinematic chains. This paper systemically investigates this 4RRR PKM's safety of homing process. A homing strategy usually contains three parts which are the home switches' locations, the platform's initial moving space, and each links' homing direction, and all of them can influence the safety of homing operation. For the purpose of evaluating and describing the safety of the homing strategy, some important parameters are introduced as follows: Safely homing ratio (SHR) is used to evaluate the probability of a machine's successfully returning home from an initial moving space; Synchronal rotational angle (SRA) is the four links' largest synchronal rotational angle with given directions from a given pose. Whether a machine can safely return home from a given pose can be judged by comparing the SRA with all four home switches' mounting angles. By meshing the initial moving space and checking the safeties of returning home from all the initial poses on the nodes, the SHR of this initial moving space can be calculate. For the sake of convenience, the platform's initial moving space should be as large as possible, and in this 4RRR PKM, a square zone in the center of the workspace with a giving initial rotation range is selected as the platform's initial moving space. The forward direction is selected as each link's homing direction according to custom, and the platform's initial rotational angle is selected as larger than 0° based on this 4RRR PKM's kinematic characteristics. The platform's initial moving space can be defined only by the side length of the initial moving square. By setting a probable searching step and calculating the SHR of the initial moving square, an optimal procedure of searching for the largest side length of the platform's initial moving square is proposed. The homing strategy proposed is based on a systemic research on the safety of homing process for PKM, and the two new indexes SHR and SRA can clearly describe the safety of homing operation. The homing operation based on this strategy is fast and safe, and the method can also be used in other PKMs with the situation of serious components' interference.

Key words: homing strategy, safely homing operation, maximum safely homing space, redundant parallel kinematic machine

1 Introduction

Kinematic model is the core part of the numerical control system, and the machine's coordinate is the base of constructing the kinematic model^[1]. If the measuring system is based on incremental encoders, the machine will lose its coordinate when it is turned off, because the incremental encoder can not save the servo-axis' position when it is out of power. So the homing process should be performed firstly to establish the machine's coordinate when the machine is startup^[2,3]. When the homing process finishes, each servo-axis should arrive at its home position. For a precise machine tool, the homing operation's success

depends on two parts: the accuracy of each axis' homing position and the safety of the operation. This paper concerns on the latter one: safety of the homing operation.

Because of the use of absolute encoders, most homing researches focus on the accuracy of homing position, few concerns with the safety of the homing operation. LIN, et al^[4], proposed a technique of using a grinding wheel as a measuring probe to determine the active parameters and the workpiece home position, their purpose is to improve a multi-axis machine tool's accuracy at the tool tip. TANG, et al^[5], calculated the homing positions of a 4-DOF hybrid machine tool's axes by kinematic calibration. DING, et al^[6], identified a 2-DOF PKM's home position and designed an experiment to verify the method. ZHANG, et al^[7], calibrated a 2RRR PKM's two active axes' homing positions by adding a redundant RRR chain. DENNY, et al^[8], proposed an interval-based method to certify whether various constraints are satisfied for all points within a required workspace and implemented it on a planar 3RRR

* Corresponding author. E-mail: liudw@mails.tsinghua.edu.cn

This project is supported by National Natural Science Foundation of China (Grant No. 50775125, and No. 50775117), National Hi-tech Research and Development Program of China (863 Program, Grant No. 2007AA041901), and National Basic Research Program of China (973 Program, Grant No. 2004CB318007)

PKM, and they obtained some useful conclusions on the relationship between the machine's constraints and the workspace. WANG, et al^[9], investigated a redundantly actuated PKM's homing strategy. By using the redundant limb, they designed an assistant homing strategy, which can not only avoid the limbs' interfere, but also help the machine pass the singular configurations during homing operation.

In this paper, a safe homing strategy is proposed for a 4RRR redundant PKM with incremental encoders. In the traditional homing mode, all servo-axes are driven independently to return to their zero positions at one time^[9]. In the traditional homing mode, the 4RRR PKM's limbs and moving platform would interfere with each other during homing. To solve this problem, a new parameter called safely homing ratio (SHR) is introduced to evaluate the safety of the homing strategy. In section 2, the 4RRR PKM's kinematic model is obtained. On the basis of the kinematic model, the platform's initial moving space, homing direction and their relations between the limbs' synchronous rotational angle (SRA) are obtained in section 3. By analyzing the difference between the three position-controlled limbs' SRA and their home switches' setting angles, the platform's largest safely homing space and homing directions are found in section 4. The SHR is used to evaluate different initial moving space's influence to the homing operation's safety. This homing strategy's design method can also be used in other PKMs with incremental encoders and with the situation of serious components' interference.

2 Structure Description and Kinematic Analysis

A safe homing strategy means that all the moving components would not interfere with each other and the terminal would not pass the singular configurations during the homing operation. To verify the safety of the homing operation, the machine's kinematic model should be obtained. The homing operation is composed of each limbs' individual homing operation. The general individual homing process is that the home switch is installed at one limit of the axis's moving space (always the positive limit), when homing, the axis will be driven towards the home switch till it triggers the switch, then moves to the zero position and stop. For a traditional machine, the movements of the links are decoupled, so the machine's homing process is simple and safe: when homing process starts, no matter where the terminal is, all the limbs execute the individual homing procedure at the same time.

2.1 Structure description

As shown in Fig. 1 (2D model) and Fig. 2 (3D model), this 3-DOF planar PKM is composed of three parts: four RRR kinematic links ($B_i-T_i-P_i$) connecting with a square base $B_1B_2B_3B_4$ and a square moving platform $P_1P_2P_3P_4$ (the

terminal). Limbs 1–3 in position control mode are used to determine the terminal's pose. Limb 4 in force control mode is a redundant limb and it is used to improve the machine's dynamic character. The machine's inputs are limbs 1–3's angles $\xi = [\xi_1, \xi_2, \xi_3]^T$ (ξ_i denotes the i th limb's rotational angle shown in Fig. 1) and limb 4's torque N_4 , the machine's output is the moving platform's pose $C = [x, y, \gamma]^T$, and it contains the position (x, y) of the platform's center point P_0 and the orientation angle γ of the platform.

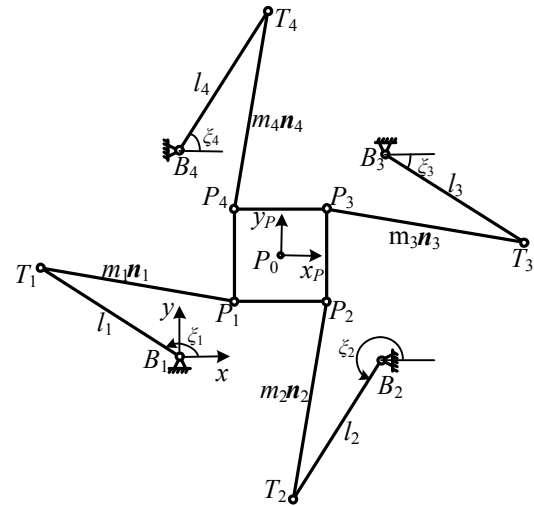


Fig. 1. The 2D model of the machine

Fig. 2. Assembly mode of the machine

The assembly mode of the machine is shown in Fig. 2, and the terminal's movement is constrained by the components' dimensions and their interferences. The kinematic analysis contains the kinematic equations and constraint equations, the former equations are used to construct the mapping model of the machine's input ξ and output C , and the latter equations are used to judge whether the input ξ or output C is available.

2.2 Inverse kinematic equation

On the basis of the terminal's closed vector chains, the machine's kinematic model can be constructed easily^[10]. The machine's two coordinates are shown in Fig. 1. The base coordinate system B - xy is fixed on point B_1 and its x

axis is along with the vector from point B_1 to B_2 . The moving coordinate system $P-x_P y_P$ is fixed on the center of the platform (P_0) with the x_P axis parallel to the vector from point P_1 to P_2 . In the base coordinate, $P_0=[x, y]^T$ denotes the position vector of point P_0 , and the position vector P_i of point P_i ($i=1, 2, 3, 4$) can be calculated as follows:

$$P_i = P_0 + R P_i^P, \quad i=1, 2, 3, 4, \quad (1)$$

where the upper script “ P ” means the vector’s value is due to coordinate system $P-x_P y_P$, else due to coordinate system $B-xy$. R is the rotational matrix from the coordinate system $P-x_P y_P$ to $B-xy$ and

$$R = \begin{pmatrix} \cos \gamma & \sin \gamma \\ -\sin \gamma & \cos \gamma \end{pmatrix},$$

where γ is the orientation angle of the moving platform. According to Fig. 1, there are four closed chains: $B_1-T_1-P_1-P_0-B_1$, $B_1-B_2-T_2-P_2-P_0-B_1$, $B_1-B_3-T_3-P_3-P_0-B_1$, $B_1-B_4-T_4-P_4-P_0-B_1$, and the following equations can be obtained:

$$P_0 = T_i + m_i n_i - P_i, \quad i=1, 2, 3, 4, \quad (2)$$

where T_i denotes the position vector of point T_i , and $T_i = B_i + (l_i \cos \zeta_i, l_i \sin \zeta_i)^T$, m_i is the length of link $T_i P_i$; n_i denotes the unit vector of link $T_i P_i$.

On the basis of Eq. (2), while the machine is in the assembly mode shown in Fig. 1, the machine’s unique inverse kinematic solutions can be obtained by cosine theorem.

The inverse kinematic equation can be written in an analytical form as

$$\xi = I(C). \quad (3)$$

2.3 Forward kinematic equation

The forward kinematic equation can not be written in an analytical form. Based on the numerical method^[11], the numerical solutions can be obtained, and the forward kinematic equation can be written as

$$C = F(\xi). \quad (4)$$

2.4 Constraint equations

The constraining equations are used to judge whether a given configuration is available. Based on the kinematic equations and the machine’s assembly mode, two constraint equations can be written as follows:

$$\varepsilon = JF(\xi), \quad (5)$$

$$\varepsilon = JI(C). \quad (6)$$

Eq. (5) is used to judge whether the limbs 1–3’s input angle $\xi_i = [\zeta_{1i}, \zeta_{2i}, \zeta_{3i}]^T$ is available, and Eq.(6) is used to judge whether the moving platform’s pose $C = [x, y, \gamma]^T$ is available. If the given configuration is available, ε would equal 1, else equal 0.

3 Analysis of the Moving Spaces

The workspaces and kinematic characterization of PKM have been studied extensively^[11,12]. Based on Eqs. (3)–(6), all the components’ moving spaces can be obtained by numerical method easily. For a homing process, its safety depends on the analysis of the terminal and all the limbs’ initial moving spaces, and while in the traditional homing mode, the safety depends on the reachable workspace of the moving platform.

3.1 Reachable workspace

Reachable workspace is the aggregate of all the positions that the terminal can arrive. The reachable workspace of the moving platform can be obtained by the inverse kinematic Eq. (3) and the constraint Eq. (6). The reachable workspace is shown in Fig. 3.

Fig. 3. Reachable workspace S_w of the terminal P_0

In Fig. 3 the center point of the reachable workspace is (353.55 mm, 353.55 mm). Define this point as the terminal’s zero position, and pose $C_0 = [353.55 \text{ mm}, 353.55 \text{ mm}, 0 \text{ rad}]^T$ as the terminal’s zero pose, and the corresponding input is $\xi_0 = [\zeta_1^0, \zeta_2^0, \zeta_3^0]^T = [2.578 \text{ rad}, 4.149 \text{ rad}, 5.720 \text{ rad}]^T$, here ζ_i^0 ($i=1, 2, 3$) denotes the i th limb’s zero position shown in Fig. 4.

Because the machine is centrosymmetric, the four limbs’ reachable workspaces are centrosymmetric too. Take limb 1 for example, design the searching procedure as follows:

Procedure 1

(1) Set the 1st limb’s rotational range: $0 \text{ rad} \leq \zeta_1 \leq 2\pi \text{ rad}$, set the incremental value of the rotational angle in each searching step, and the 1st limb’s rotational angle is

denoted by ξ_{li} .

(2) Set the rotational ranges of angle $\angle B_1T_1P_1$ and $\angle T_1P_1P_0$ in the 1st kinematic chain: $0 \text{ rad} \leq \angle B_1T_1P_1 \leq \pi \text{ rad}$, $\pi/4 \text{ rad} \leq \angle T_1P_1P_0 \leq 7\pi/4 \text{ rad}$. Set the value of the incremental angle in every searching step, and σ_n denotes the value of angle $\angle B_1T_1P_1$, τ_m denotes the value of angle $\angle T_1P_1P_0$.

(3) On the basis of the angles $(\xi_{li}, \sigma_n, \tau_m)$ given in steps 1 and 2, the platform's pose $C_{li} = [x_{li}, y_{li}, \gamma_{li}]^T$ can be calculated. Load C_{li} into Eq. (6) to judge whether C_{li} is available. Check every ξ_{li} defined in step 1, if there exists an available pose C_{li} , save ξ_{li} .

(4) When finish checking all the angles of ξ_{li} defined in step 1, the 1st limb's rotational range can be obtained, that is the 1st limb's reachable workspace L_{w1} . The rest three limbs' reachable workspaces can be obtained by the law of symmetry.

The reachable workspaces of all the limbs are shown in Fig. 4. In Fig.4 the shadow regions are the reachable workspaces: $0.0427 \text{ rad} \leq \xi_1 \leq 5.6346 \text{ rad}$, $1.6135 \text{ rad} \leq \xi_2 \leq 7.2054 \text{ rad}$, $-3.0988 \text{ rad} \leq \xi_3 \leq 2.4930 \text{ rad}$, $-1.5280 \text{ rad} \leq \xi_4 \leq 4.0638 \text{ rad}$, and $\text{lim}+$ denotes the positive limit, $\text{lim}-$ denotes the negative limit.

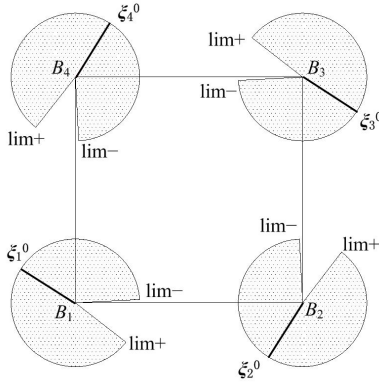


Fig. 4. Limbs 1–4's reachable workspaces L_{wi} ($i=1, 2, 3, 4$)

3.2 Limbs 1–3's synchronal rotational angle (SRA)

Define limb 1–3's synchronal rotational angle (SRA) as follows: while limb 1–3 rotate in the same velocities, and at the same time, the maximum angle they can rotate is their synchronal rotational angle. SRA is a useful parameter for the homing design. The value of SRA depends on limb 1–3's rotational directions D and the terminal's pose C . Its calculation equation is shown as follows:

$$r_{\text{SRA}} = S_{\text{SRAI}}(C, D) = S_{\text{SRAF}}(\xi, D), \quad (7)$$

where $C = [x, y, \gamma]^T$, $\xi = I(C)$, $D = [d_1, d_2, d_3]^T$, d_i denotes the i th limb's rotational direction, and if the rotational direction is positive, $d_i = 1$, otherwise $d_i = 0$, $i = 1, 2, 3$.

The machine's homing direction is the limbs' rotational directions when homing process starts. Generally, the machine's homing direction is positive, thus $D_h = [1, 1, 1]^T$ while homing process starts.

4 Design of the Homing Strategy

In the homing process, all limbs are directly controlled by the servodriver to return to their zero positions independently, so each limb's rotational speed and direction are changeless during homing.

For a redundantly actuated PKM, there is another thing should be paid attention to: the redundant limb has a restriction on other limbs during homing. The restriction should be released in the homing process, and an effective way is letting the redundant limb be controlled by a force mode in which the force command value is zero^[9]. Now the machine's homing process is only composed of limb 1–3's individual homing operations, and a safe homing process means the safe individual homing process of limbs 1–3.

The individual homing process can be divided into three steps as follows:

(1) When homing process starts, the limb moves in a specified direction (towards the home switch's position).

(2) After the limb is triggered the home switch, it keeps on moving and the axis' servodriver starts searching for the encoder's reference mark.

(3) While finding the reference mark, the limb stops, then rotates a specified angle and stops again, and the final position is the limb's zero position.

So a safe individual homing process depends on the limb's rotational speed and direction, the limb's initial rotational space and the home switch's stopping position.

For convenience, in this machine's homing process, let all the limbs rotate in the same speed and all in positive direction, so the home switches are installed at the positive limits of the limbs' initial moving spaces. Now the safety of homing process depends only on three parts: the terminal's initial moving space, the terminal's initial rotational range, and whether the machine passes the singular configurations during homing.

4.1 Basic definitions

To evaluate the safety of homing operation, define the corresponding variables as follows.

(1) S_{init} —The initial moving space of the terminal P_0 which is all possible positions' aggregate of the terminal P_0 before homing.

(2) $L_{\text{init-}i}$ —The initial rotational space of the i th limb which is all possible rotational angles' aggregate of the i th limb before homing. $L_{\text{init-}i}$ depends on S_{init} and the terminal's initial orientation range. $\text{lim}+_i$ denotes $L_{\text{init-}i}$'s positive limit and $\text{lim}-_i$ denotes the negative limit.

(3) Safely homing point with the terminal's rotational range θ —If the machine can return home safely at point (x, y) with every available orientation angle γ inside the rotational range θ ($\gamma \in \theta$), this point (x, y) is called the safely homing point with the terminal's rotational range θ . The aggregate of these points is denoted by M and can be seen as the safely homing space with the terminal's rotational range θ .

(4) SHR—Safely homing ratio which is the value of S_0/S_{init} , and S_0 denotes the safely homing space. SHR depends on S_{init} , θ and the homing direction \mathbf{D}_{home} , thus $R_{\text{SHR}} = S_{\text{SHR}}(S_{\text{init}}, \theta, \mathbf{D}_{\text{home}})$.

When given S_{init} , θ and $\mathbf{D}_h = [1, 1, 1]^T$, R_{SHR} can be calculated by the following procedure.

Procedure 2

(1) Calculate limb 1–3's initial moving spaces $L_{\text{init-}i}$ ($i=1, 2, 3$) and get their home switches' stopping positions $\omega = [\omega_1, \omega_2, \omega_3]^T$, where ω_i denotes the home switch's position of the i th limb and $\omega_i = \text{lim} +_i$ ($i=1, 2, 3$).

(2) Set the mesh spacing and mesh the terminal's initial moving space S_{init} . The aggregate of the nodes is denoted by \mathbf{N} .

(3) Set the incremental step size of the terminal's orientation angle, and obtain the terminal's all available poses $\mathbf{C}_{i-j} = [x_i, y_i, \gamma_{i-j}]^T$ at node $N_i = (x_i, y_i)$, where $N_i \in \mathbf{N}$, $i=1, 2, \dots, \text{num}(\mathbf{N})$, $\gamma_{i-j} \in \theta$, $\text{num}(\mathbf{N})$ denotes the number of \mathbf{N} 's elements.

(4) Based on Eq. (3) and Eq. (7), while the pose is \mathbf{C}_{i-j} , the corresponding input $\xi_{i-j} = [\xi_{1i-j}, \xi_{2i-j}, \xi_{3i-j}]^T$ and the synchronal rotational angle $r_{\text{SRA}i-j}$ can be obtained.

(5) $\max(\omega_i - \xi_{1i-j})$ denotes the maximum value of $\omega_i - \xi_{1i-j}$ ($i=1, 2, 3$). If $r_{\text{SRA}i-j} \geq \max(\omega_m - \xi_{mi-j})$ ($m=1, 2, 3$) in every pose \mathbf{C}_{i-j} defined in step 3, and all the traverse poses during homing are not singular configurations, node N_i is a safely homing point.

(6) Check every node $N_i \in \mathbf{N}$ ($i=1-\text{num}(\mathbf{N})$) to find all the safely homing points, and their aggregate is \mathbf{M} , then $R_{\text{SHR}} \approx \text{num}(\mathbf{M})/\text{num}(\mathbf{N})$.

For the traditional homing strategy, the terminal's initial moving space is the reachable workspace $S_{\text{init}} = S_w$ (Fig. 3), and the terminal's initial rotational range $\theta_w = [0, 2\pi]$, the homing direction $\mathbf{D}_h = [1, 1, 1]^T$. Based on procedure 2, the traditional homing strategy's R_{SHR} can be calculated and $R_{\text{SHR}} = 0$, and that means the machine can not return home at any point in the reachable workspace.

From procedure 2, we can find that the success of homing depends on S_{init} , θ and \mathbf{D}_h . When $\mathbf{D}_h = [1, 1, 1]^T$, there are two ways to make the homing process success: reduce the terminal's initial space S_{init} , and reduce the terminal's initial rotational range θ . The following sections will investigate S_{init} and θ 's influences on SHR and will find an efficient homing strategy.

4.2 Effect of the terminal's rotational range θ

At any position, the terminal's orientation angle γ has an effect on $\xi = [\xi_1, \xi_2, \xi_3]^T$. Take the center point (353.55 mm, 353.55 mm) as an example, the machine's configurations are shown in Fig. 5 while the terminal's rotational angle $\gamma = 20^\circ, 0^\circ, -20^\circ$.

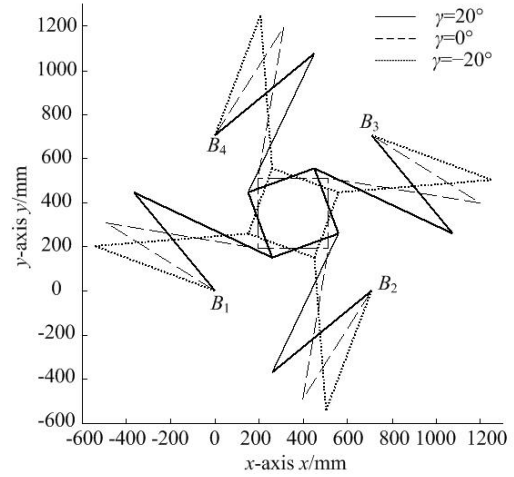


Fig. 5. γ 's effect on ξ at (353.55 mm, 353.55 mm)

From Fig. 5, we can find that, when the terminal is at the point (353.55 mm, 353.55 mm), a smaller ξ_i ($i=1, 2, 3$) corresponds to a larger γ and the same conclusion can be obtained at any other points.

From step (5) of procedure (2), we can find that for a safely homing process in a pose \mathbf{C} , r_{SRA} must be greater than $\max(\text{lim} +_i - \xi_i)$ ($i=1, 2, 3$), while \mathbf{C} is given, r_{SRA} and ξ_i are changeless, thus the only way is to decrease $\text{lim} +_i$ of each limb's initial moving space. The following conclusions can be drawn: In the same initial moving space, the terminal's orientation angle γ should be as larger as possible. So for an easier operability, let $\gamma > 0$ before homing operation.

4.3 R_{SHR} of the initial moving space S_{init}

For convenience, suppose that the S_{init} is a square region in the center of the workspace with one side parallel to x -axis, and the length of its side is t . A safely homing place means any inside point is a safely homing point, so to check whether a place is the safely homing place, every inside point should be checked. Procedure 3 is designed to search the maximum t as follows.

Procedure 3

(1) Mesh the initial moving space S_{init} , and the aggregate of the nodes is denoted by \mathbf{K} . $\mathbf{K}_i = (x_i, y_i)$ denotes one element of \mathbf{K} , and $353.55 - t/2 \leq x_i \leq 353.55 + t/2$, $353.55 - t/2 \leq y_i \leq 353.55 + t/2$.

(2) Set the incremental step size of the terminal's orientation angle and get the terminal's all available poses $\mathbf{C}_{i-j} = [x_i, y_i, \gamma_{i-j}]^T$ at the node \mathbf{K}_i ($\mathbf{K}_i \in \mathbf{K}$, $\gamma_{i-j} > 0$).

(3) Check every pose \mathbf{C}_{i-j} defined in step 2, if all of them are safely homing poses, save \mathbf{K}_i .

(4) Check every node $\mathbf{K}_i \in \mathbf{K}$, find all the safely homing points, and their aggregate is \mathbf{G} . Then $R_{\text{SHR}} \approx \text{num}(\mathbf{G})/\text{num}(\mathbf{K})$.

The results are shown in Table 1.

Table 1. R_{SHR} of different initial moving spaces

Parameter	Value						
Side length t /mm	≤ 48	50	60	70	80	90	100
Initial moving space S_{init}/mm^2	≤ 2	304	2 500	3 600	4 900	6 400	8 100 10 000
Safely homing space S_0/mm^2	S_{init}	2 421	2 581	2 042	1 353	604.3	0.5
Safely homing ratio R_{SHR}	100%	96.8%	71.7%	41.7%	21.1%	7.5%	0

The safely homing spaces are shown in Fig. 6, and the white region inside the square is the safely homing space. t is changed from 0 mm to 120 mm to calculate the value of safely homing ratio (R_{SHR}) is shown in Fig. 7.

From the t - R_{SHR} curve shown in Fig. 6, we can find that $R_{SHR}=1$ when $t \leq 48$ mm. The maximum safely homing space S_{0-max} is a square region with the side-length equal 48mm, and it is in the center of the base $B_1B_2B_3B_4$ with its sides parallel to B_1B_2 or B_2B_3 .

When $S_{init}=S_{0-max}$, the positive limits of limb 1-3's rotational ranges are $lim_{+1}=2.695$ rad, $lim_{+2}=4.266$ rad, $lim_{+3}=5.836$ rad. Obviously, S_{0-max} is the terminal's optimal initial moving space before homing, and if the input is close to $\zeta=[2.695$ rad, 4.266 rad, 5.836 rad]^T the homing speed would be fast. To ensure each limb can trigger the home switch in a fast speed, $\xi=[2.575$ rad, 4.146 rad, 5.716 rad]^T is a suitable input before the machine shutdown, and the corresponding pose is $C=[353.466$ mm, 353.451 mm, 0 rad]^T.

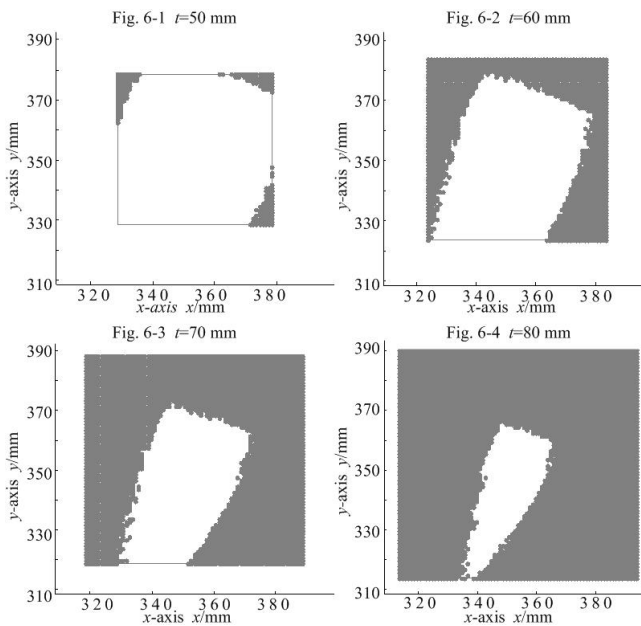


Fig. 6. Safely homing spaces

Fig. 7 t - R_{SHR} curve

4.4 Homing Strategy

By now, the 4RRR PKM's homing strategy can be obtained as follows.

(1) Set the home parameters (Fig. 8) stored in the servodrivers: limbs 1-3's homing directions are all positive, and are all in the same speed with a suitable value. When triggering the home switch, each link stops and rotates -0.116 rad, then stops again.

(2) Install the home switches at suitable positions with the following angles: $\omega_1=2.695$ rad, $\omega_2=4.266$ rad, $\omega_3=5.836$ rad.

(3) Before shutdown, stop the machine in pose $C=[353.466$ mm, 353.451 mm, 0 rad]^T, this is named the shutdown pose.

(4) Before homing operation, check the pose of the terminal: make sure the position is within the safe homing space S_{0-max} , and the orientation angle γ is positive.

The final homing parameters are shown in Fig. 8.

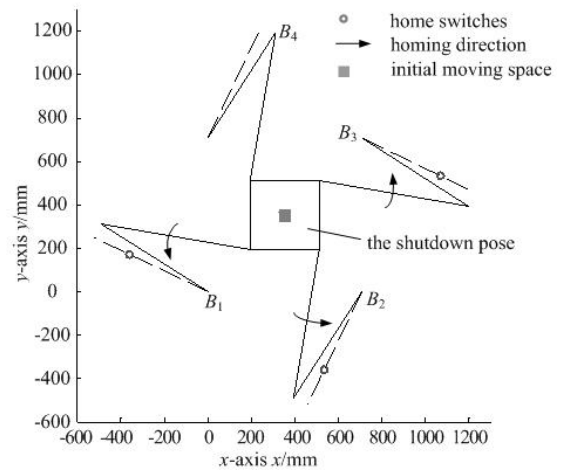


Fig. 8. Final homing parameters

5 Conclusions

(1) For a machine, if the kinematic chains' motions couple severely, the traditional homing method is usually unusable, and the limbs' synchronal moving space can be used to evaluate the coupling level.

(2) The constraint equation depends on not only the

components' dimensions, but also the machine's assembly mode, and the solution of the equation can be used to judge whether the pose is available.

(3) Homing strategy of all the limbs' synchronal homing operation is fast and simple, but the terminal's initial pose should be limited in a special region. Stopping the terminal in a specified pose by numerical control system before the machine's shutdown is a feasible way.

(4) The terminal's orientation angle has a large influence on all the limbs' rotational angles, and the constraint of the initial orientation angle depends on the individual homing directions of all the limbs.

(5) Safely homing ratio (SHR) is an effective parameter to evaluate the safety of the homing strategy, and depends on the terminal's initial moving space and initial rotational range. The terminal's initial moving space should be as large as possible while $R_{SHR}=1$.

References

- [1] DAVID Gibbs, TMOMAS M Crandell. *An introduction to CNC machining and programming*[M]. New York: Industrial Press, 1991.
- [2] CHEN Junlong. *Numerical control and numerically controlled machine tool*[M]. Hangzhou: Zhejiang University Press, 2007. (in Chinese)
- [3] ZHANG Shu, HERSEL U. *Parallel kinematics machine tool*[M]. Beijing: China Machine Press, 2003. (in Chinese)
- [4] PSANG Dain Lin, CHIAN Sheng Tzeng. Modeling and measurement of active parameters and workpiece home position of a multi-axis machine tool[J]. *International Journal of Machine Tools and Manufacture*, 2008, 48(3-4): 338-349.
- [5] TANG Xiaoqiang, LI Tiemin, YIN Wensheng, et al. Accuracy analysis and calibration of gantry hybrid machine tool[J]. *Tsinghua Science and Technology*, 2003, 8(6): 702-707.
- [6] DING Qingyong, SUN Lining, JI Junhong. Calibration of a 2-DOF planar parallel robot: Home position identification and experimental verification[C]//*IEEE International Conference on Mechatronics and Automation*, Niagara Falls, Ontario, Canada, 29 July-1 Aug, 2005: 510-515.
- [7] ZHANG Yaoxin, CONG Shuang, LI Zhexiang, et al. Auto-calibration of a redundant parallel machine based on the projected tracking error[J]. *Archive of Applied Mechanics*, 2007, 77(10): 697-706.
- [8] DENNY Oetomo, DAVID Daney, Shirinzadeh, BIJAN Shirinzadeh, et al. Certified workspace analysis of 3RRR planar parallel flexure mechanism[C]//*IEEE International Conference on Robotics and Automation*, Pasadena, CA, USA, May 19-23, 2008: 3 838-3 843.
- [9] WANG Jinsong, WU Jun, WANG Liping, et al. Homing strategy for a redundantly actuated parallel kinematic machine[J]. *Journal of Mechanical Design*, 2008, 130(4): 1-5.
- [10] CHANG Peng, WANG Jinsong, LI Tiemin, et al. Step kinematic calibration of a 3-DOF planar parallel kinematic machine tool[J]. *Science in China Series E-Technological Sciences*, 2008, 51(12): 2 165-2 177.
- [11] WANG L T, CHEN C C. On the numerical kinematic analysis of general parallel robotic manipulators[J]. *IEEE Transactions on Robotics and Automation*, 1993, 9(3): 272-285.
- [12] KUMAR Vijay. Characterization of workspaces of parallel machines [J]. *ASME J. Mech Des*, 1992, 114(3): 368-375.
- [13] GOSELIN C. Determination of the workspace of 6-DOF parallel machines[J]. *Journal of Mechanical Design*, 1990, 112(3): 331-336.

Biographical notes

WANG Liping, born in 1967, is currently a professor and a PhD candidate supervisor in *Tsinghua University, China*. His research interests include advanced manufacturing equipment and control, numerical control technology and parallel kinematic machine. Tel: +86-10-62796876; E-mail: lpwang@tsinghua.edu.cn

LIU Dawei, born in 1984, is currently a PhD candidate in *Department of Precision Instruments and Mechanology, Tsinghua University, China*. His research interests include the accuracy analysis and calibration of parallel kinematic machine. Tel: +86-10-62781820; E-mail: liudw_thu@163.com

LI Tiemin, born in 1971, is currently an associate professor in *Tsinghua University, China*. His research interests include parallel kinematic machine design, robot mechanics, accuracy analysis and calibration of parallel kinematic machine and redundant parallel kinematic machine. Tel: +86-10-62792792; E-mail: litm@tsinghua.edu.cn